UNIVERSITY OF CALIFORNIA
RIVERSIDE

Quantifying Changes to the 3D Structure of Microglia in Response to an Insult from Inhalation of *Alternaria Alternata* Particulate Matter

A Thesis submitted in partial satisfaction
of the requirements for the degree of

Master of Science

in

Biomedical Sciences

by

Chigozie C. Okeke

June 2021

Thesis Committee:
Dr. Monica J. Carson, Chairperson
Dr. Byron D. Ford
Dr. Sika Zheng

The Thesis of Chigozie C. Okeke is approved:

_____

_____

_____

Committee Chairperson

University of California, Riverside

Acknowledgements

I wish to extend my special thanks to the Carson Lab, and my family

ABSTRACT OF THE THESIS

Quantifying Changes to the 3D Structure of Microglia in Response to Insult from Inhalation of *Alternaria Alternata* Particulate Matter

by

Chigozie C. Okeke

Master of Science, Graduate Program in Biomedical Sciences
University of California, Riverside, June 2021
Dr. Monica J. Carson, Chairperson

Continuous exposure to aerosolized allergens leads to the activation of the innate and adaptive immune system in the lung. Systemic inflammation in peripheral tissues has the potential to trigger activation of the brain's resident immune cell, the microglia. Here we test whether airborne exposure to a common allergen, *Alternaria alternata* for 7 days at levels sufficient to trigger lung inflammation is sufficient to trigger activation or changes in homeostasis of microglia within the learning and memory region of the murine brain (the hippocampus). We specifically quantify the morphological structure of microglia in the hippocampus CA1 region by performing Sholl analysis on microglia visualized with antibodies against IbaI using the Neurolucida®360 software. Analysis revealed an increase in microglial process length in both sexes of mice exposed to allergen. However, a shift in morphology associated with reactive activation of microglia was only observed in female mice exposed to allergen. These data suggest that airborne

exposure to a natural fungal allergen is sufficient to cause changes in hippocampal brain tissue that are different between sexes, with microglia in exposed females being more responsive than microglia in exposed males.

Table of Contents

List of Figures

Introduction

Infection is a large area of study with multiple facets of study from the immune mechanisms of different compartments in the body, to the study of the effects of various antigens on the body, to the interplay between both the adaptive and innate immune system. From these various studies it has been concluded that the introduction of an antigen into one part of the body can have a systemic effect on base homeostasis. Various insults can trigger this systemic reaction depending on the antigen, and the method of administration. My research focuses on a widely applicable insult and reaction paradigm. Allergies are faced by a large portion of the U.S population, according to a 2018 CDC summary over 19.2 million adults were diagnosed with hay fever in the 12 past months. Another 2019 survey estimated about 8% of adults and 7% of children have asthma (National Center for Health Statistics 2019; National Asthma Data 2019). Many allergens whether natural or man-made, are often aerosolized and enter the body through inhalation leading to a reaction. My research focuses on analyzing changes in the brain because of this inflammation. As previously stated, insults by antigens may be localized but have an overall systemic effect on the body. For allergens pulmonary inflammation is a direct result of allergen inhalation but can manifest first as allergic rhinitis commonly known as hay fever a mild and localized reaction to allergen particulates. Symptoms can widely vary from trouble breathing, to irritation of the eyes and throat, to fatigue. Continuous/prolonged exposure can lead to more severe outcomes such as in asthma where we see a systematic response in T-cell proliferation, and cytokine modulation (Bartemes et al., 2018). People who suffer from both allergic rhinitis and asthma have

described a hazy/tired felling which makes it hard for them to concentrate leading to instances of lost time; colloquially known a “brain fog”.

In animal model systems chronic exposure to allergens has revealed an impact in behavioral alterations such as impaired learning and memory in the Morris water maze, disturbed long-term potentiation in the hippocampal CA1 region, and reduced hippocampal cell proliferation (Guo et al., 2013; Klein et al., 2016; Peng et al., 2018). In one study, C57Bl/6J mice exposed for 96hrs continuously to the allergen *Alternaria alternata* were subsequently sacrificed and had their lung and brain tissue analyzed. From this analysis there was found to be physiological changes such as an increase in BAL count, alveolar macrophage count, and similar pathology score to intranasal Alternaria dosing indicating that aerosol exposure to Alternaria was sufficient to produce pulmonary inflammation (Peng et al., 2018). Furthermore, qPCR analysis of whole brain homogenate excluding medulla by the same study showed trending differences in neuroinflammatory molecules such as lower Arginase 1 and NOX2; higher iNOS and TNFα levels. qPCR analysis of medulla homogenates showed significantly lower Arginase 1, iNOS, and TNFα levels.

For our research, we induced changes in the CNS by exposure to aerosolized Alternaria using a specialized chamber where clean air was pumped into a suspension of Alternaria liquid which was atomized and passed through a heating coil and dryer to diffuse into the chamber (Peng et al., 2018). A cage was placed in this chamber and C57Bl/6J mice were continuously exposed for a total of 7 days. From this the route of administration for our allergen was through natural inhalation.

Alternaria is a common allergen found on various types of vegetation and is widely present as an inhalant in spores that can be found both indoors and outdoors (Knutsen et al., 2012; Gabriel et al., 2016). Alternaria is considered a general health risk as it readily triggers immune sensitization and is a primary risk factor in the development of asthma. Exposure to previously sensitized individuals is correlated with a severe risk of morbidity and a higher risk of fatal asthma attacks. In conjunction with being one of the most abundant sources of airborne allergens and being found sufficient to produce quantifiable changes to neuroinflammation markers in the brain in a shorter exposure time, Alternaria was a great candidate for our study (Bush and Prochnau, 2004; Knutsen et al., 2012; Gabriel et al., 2016; Vianello et al., 2016; Peng et al., 2018).

In the brain, we were looking for any indication of physiological changes in response to Alternaria exposure. To this end, we decided to look at regions of hippocampal CA1 close to the stratum radiatum. The reason we were looking in the CA1 hippocampus is due to the aforementioned “brain fog”. With affected individuals reporting symptoms of losing time, we hypothesized that this would be due to changes in the brain that result in a failure to properly encode events in memory, which is centralized in the hippocampal structure. Added to studies that have shown impaired learning and memory and affected long-term potentiation, the hippocampus was a natural place to look for physiological changes. As a readout of these changes, we decided to look at microglial morphology. Microglia are the resident macrophages of the CNS found in the brain and the spinal cord. They are responsible for many functions such as removing damaged neurons, removing infections, phagocytosis of cellular debris, regulation of inflammation, and

antigen presentation. As a result of their wide variety of functions, microglia are very plastic and sensitive to their surrounding environment. In homeostatic immune tissue, microglia are in a non-reactive or ramified state where their processes survey a defined area constantly. However, the cell itself may not have much or any movement and secrete fewer immunomolecules. In contrast, when processes detect sufficient environmental stimuli, microglia shift into a more reactive state, that gives them an ameboid shape. Some of the hallmarks of reactive microglia are the retraction and thickening of its processes, which in consequence leaves less of the immediate brain surveyed (Jonas et al., 2012). Microglial cell bodies swell indicating the creation of more signaling molecules and substances seen the increased granules. Reactive microglia may also become more motile.

With a change in morphological structure being one of the hallmarks of reactive microglia, these changes can be measured using Sholl analysis. Sholl analysis is a quantitative method by where different parameters of a cell's morphology can be measured through a concentric shell method. Where within each shell starting from the soma different parameters are measured and plotted against the increasing radius. This will tell us how ramified the microglia become in response to our Alternaria insult. Our research focused on developing the method for measuring the ramification of microglia using built in 3D Sholl analysis tools in the Neurolucida®360 and Neurolucida® Explorer software with 3D slices.

Method

To produce the microglial cells for tracing, mice were raised to either two months or 21 days. After this time, the mice in the experimental group were put in a chamber where aerosolized Alternaria was introduced. These mice were kept there for a certain amount of time per day for 7 days. This contrasts with the control group which was exposed to regular vivarium conditions for the entire experiment. After the seven-day experiment was complete the mice were sacrificed, and brain tissue collected. Sagittal cuts were made to examine effects of Alternaria insult on the CA1 region of the hippocampus. The collected tissue was stained with Iba1 antibody to visualize microglia and their processes while DAPI was used to visualize the nucleus. After the staining and fixation each sample was loaded onto a plate and preserved until analyzed using a confocal microscope. Each slice of tissue was subdivided into three fields for analysis. Each field was further divided into four quadrants and ideally one microglial cell was chosen from quadrants one to three for 3D analysis. For each condition divided by sex, a total of three biological replicate animals were used and at least two microglia from each field were captured. This sampling method gives a sample of at least six cells per tissue per animal, and with three animals gives a minimum of 18 cells per condition.

Each microglial cell was captured as a 3D image and to be analyzed had to first be converted from its raw image file into a format compatible with Neurolucida 360 and Neurolucida Explorer. Images were converted into uncompressed .tiff files using FIJI (Image J). For automated analysis with the program the following steps were conducted:

1.When opening the image file in Neurolucida set the thickness to 0.37 micrometers with an x, y positioning of 0.087819. This sets the voxel size for the 3D environment by scaling the micrometer to voxel ratio.

2.When locating the soma set the size parameters to a min ('Size Constraint') of 2 and a max ('Interactive Search Region') of 13; set the sensitivity ('Soma Detector Sensitivity') to 75% and hit 'Detect All Somas'.

●The settings are what was found to work best through trial and error

3.When the program is finished select the excess soma and delete them. To do this hit 'Edit' and then manually select the soma you want to delete and hit 'Delete' on the keyboard. You can select multiple somas by holding 'Ctrl' as you select them

4. After selecting the targeted microglial soma and set the transparency to 50% using the slider

5.Examine where the program detects the soma to be, this is because sometimes it might not include all the soma or too much, if this happens either:

a. reduce the sensitivity (+/- 10%)

b. increase the sensitivity (+/-10%)

6. After this set the program to "automatic" in tracing mode and selected voxel scooping from the tracing methods below:

i. Directional kernels: good for images where you trace long processes that are approximately one continuous line

ii. Crawling rayburst: which is good for tracing processes that have variable borders

iii. Scooping voxel: which is good for images that have a high contrast between the subject and the background

7. Below in the display seeds tab we set the sensitivity to 80 and the density to “dense” giving enough seeds for an accurate tracing but limiting the number of false seeds where no processes were located.

8. In the refine seeds tab the refine filter allows you to set the tolerance for seeds detected by the program. Two was found to be the optimal setting for these tracings. Extraneous seeds were removed with the “remove seeds with circular cursor” option.

9. In the trace tab sensitivity was set to 82 and gap tolerance was set to the maximum “large”. Both the “remove traces shorter than” and “connect branch segments” options were enabled. The remove trace value is generated by the parameters of the tracing automatically using the Neurolucida®360 software to be consistent

10. In the advanced settings seed detection was set to dense

11. Under tracing both detector options are enabled with super-ellipsoids set to 20 iterations and “always”. “Detector size range in pixels” should have the minimum set to 10 and the maximum set to 18. For “detector movement constraints” rotation should be set to 9 and shifting to 3.

12. For branch connections “largest gap” is auto-generated to maintain consistency throughout the tracings “deviation angle” was set to 79 degrees for the same reason, and a “minimum ratio of” was set to 22%.

13. After completing step 12 and tracing click the ‘Save and view in Neurolucida Explorer’ button that should bring up a 3D display of the tracing in the new program.

14. Go to Analyze ->Spatial -> Sholl Analysis and set starting radius at 10µm, and radius increment at 5µm; with a ‘Line Thickness’ of 1. Check ‘Dendrites’ under Analysis and hit ‘Display’

15. The return should be a matrix readout. Copy this information and put into an appropriate data sheet for analysis and statistics.

Results

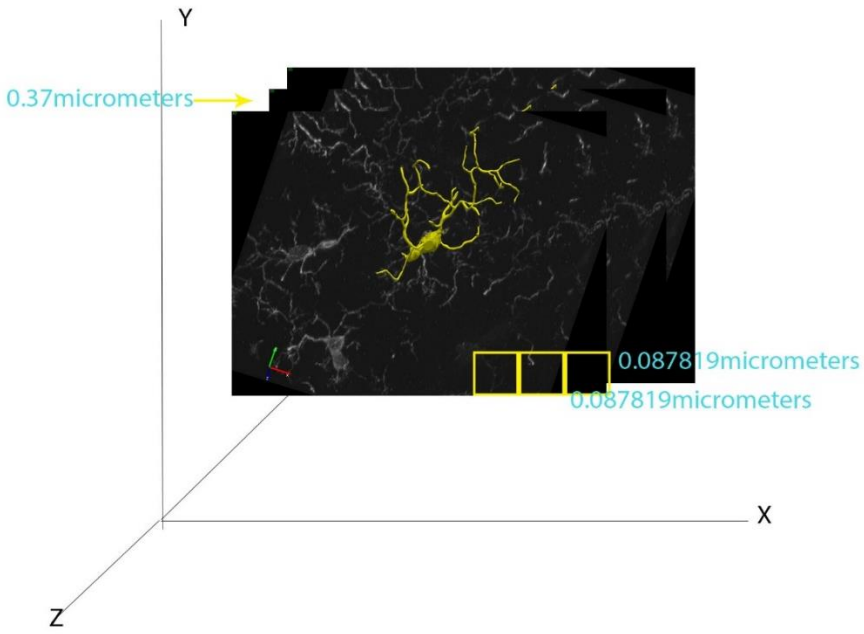

Figure 1. Schematic of 3D microglia reconstruction. 3D reconstruction done in Neurolucida®360 using images taken from a microscope as a Z-stack. Raw images were processed using ImageJ. Each pixel is set to represent an area of .087819μm x .087819μm. Each voxel is set to represent a volume of .087819μm x .087819μm x .37μm

In response to changes in brain tissue environment microglia can respond in a multitude of ways including changes to their morphology, such as soma size, and branching complexity. In Figure 1, we outline in yellow one microglia from the multiple in this slice of tissue to measure these morphological changes using Sholl's analysis. Sholl's analysis is a quantitative measure of the morphological changes of imaged neuronal cells. To use this technique for our purposes targeted microglia had to have a labeled soma, clearly labeled processes, and have only one centered microglia.

The collected tissue was stained with Iba1 antibody to visualize microglia and their processes; DAPI was used to visualize the nucleus. After the staining and fixing process each sample was loaded onto a plate and preserved until analyzed at the confocal microscope. Each slice of tissue was subdivided into three fields for analysis. Each field was further divided into four quadrants and ideally one microglial cell was chosen from quadrants one to three for 3D analysis. For each condition divided by sex a total of three biological replicate animals were used; from these animals at least two microglia from each field were captured. This sampling method gives a sample of at least six cells per tissue per animal, and with three animals gives a minimum of 18 cells per condition.

The analyzed cells were taken at a 63x magnification and were all set to the same three-dimensional measurements for Sholl's analysis. As shown in the figure above every analyzed cell consisted of multiple stacked pictures taken of the same cell at different depths on the z-axis. For each of the pictures the dimensions had to be set in the Neurolucida program converting cubic micrometers into voxels for analysis. Each voxel is a three-dimensional space that is defined by the researcher that took the picture. For our photos, each voxel is defined by a z-axis of 0.37 μm and an x/y-axis that is an inverse of the scope settings. This turned out to be .087819μm for each axis. In summary each voxel defined by the xyz axis is .087819μm x .087819μm x .037μm in the program. The combination of these stacked pictures creates a three-dimensional representation of the target microglia and the area around it.

Each 63x magnified field was centered on microglia (highlighted in yellow) for Sholl analysis, but it also shows the surrounding processes and soma for in field and out of

field microglia. The built-in tools for analysis of the microglia depend on the definition of a voxel for tracing of processes and collecting of data such as thickness, length, volume, etc. This presents the problem of how to separate the microglial measurements that we are interested in from the surrounding background.

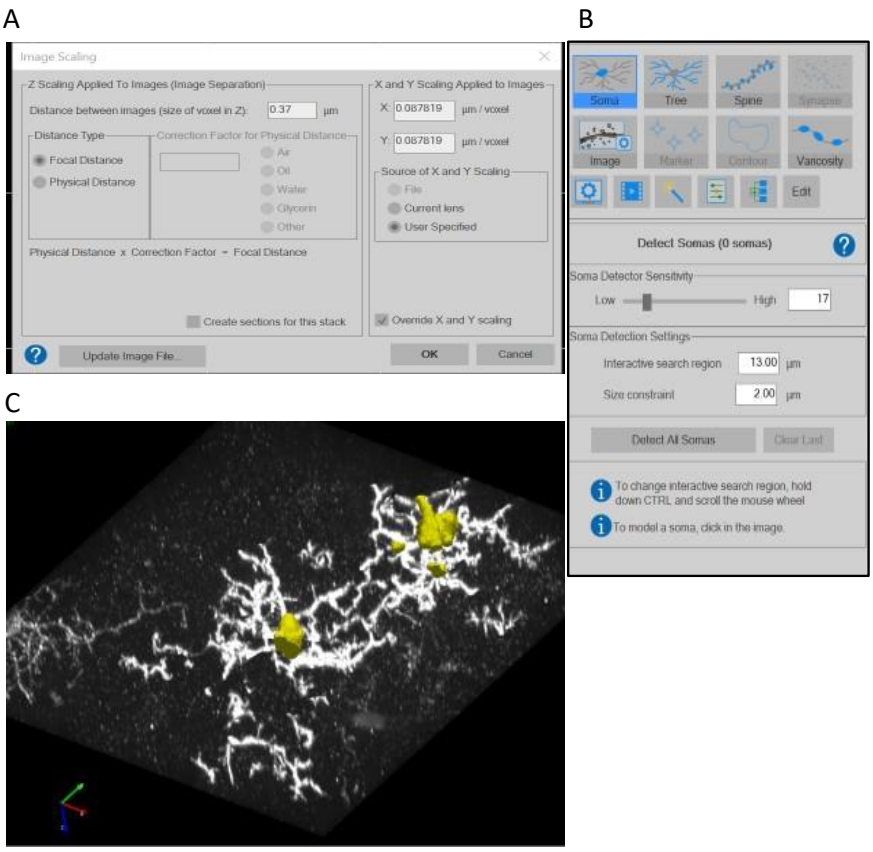

Figure 2. Set up of 3D reconstruction and soma processing using Neurolucida®360. (a) Image scaling used to create the 3D reconstruction in the program. (b) Dialogue box used for detection of microglial somas in 3D reconstruction. (c) Example of completed soma detection in a 3D reconstruction.

In Figure 2 we show the process of setting the soma detection parameters and the image scaling parameters within the program. When first opening the .tiff file in Neurolucida 360 the first prompt in panel A is presented. Here we had to set the scaling for the image file. This scaling would give us an accurate representation of the stained microglia and surrounding environment with the various objects to scale. These settings were based off the lens setting used when imaging the slides. Each image was taken to a depth of about 2 μm for the z axis and a length/width of about 12μm for the x and y axes so to calculate

the μm/voxel ratio is just the formula $\frac{1}{x}$. With this we have one voxel representing a volume of $(0.087819 * 0.087819 * 0.37)\mu m^3$.

Figure 2A shows the automatic soma detection method that was used in the process. For this tool three parameters must be defined. Size constraint refers to the minimum size that the program will look for when considering what qualifies as a soma. This was set to $2\mu m$ as this setting gave the best results in detecting all somas in the projection. Interactive search region sets the maximum range from the center of the 3D projection that the program will search in finding somas. This was set to $13\mu m$ to tell the program to search the whole projection for potential somas. The soma detector sensitivity was set to a range from 70-82 as this gave the best results in tracing all the contours and ridges of most microglial somas imaged as shown in Figure 2B and 2C.

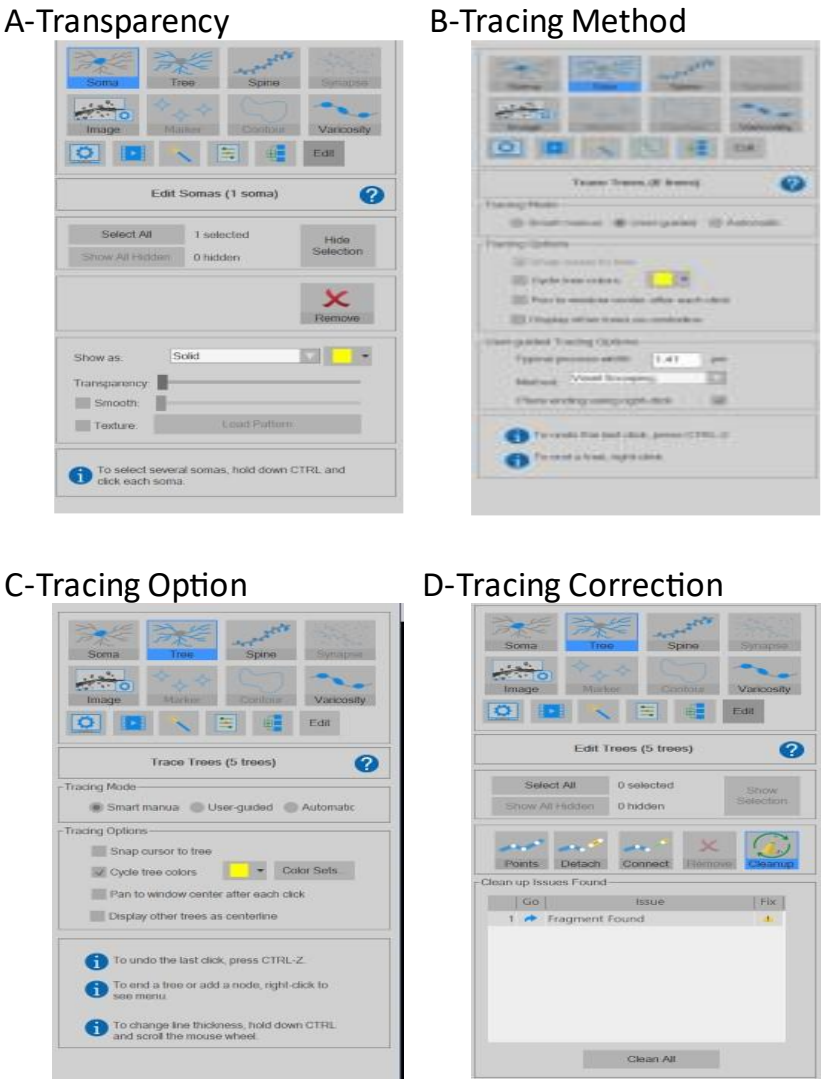

Figure 3. Array of dialogue boxes used for soma detection and process tracing. (a) Options to change the transparency of the soma detection marker. (b) Settings for the tracing options to determine mode of the program. (c) Settings for tracing options. (d) Settings for correcting errors within the tracing.

Figure 3 shows the built-in checks for soma detection and the parameters for tracing of the processes following the original software-assisted hand tracing method. In figure 3A the software options for the soma are displayed. To ensure that the soma detection

algorithm used in Figure 2 labeled the soma in its completeness the opacity of the labeled soma was set to 50%. Depending on the coverage the sensitivity (Figure 2) was adjusted accordingly by increments of ±10% until the labeled soma did not include the processes of the microglia.

Figures 3B/C outline the setup process for the software-assisted tracing of microglia processes. The tracing mode was set to user-guided and in the tracing options 'snap cursor to tree' was enabled to keep the tracing centered on one projection at a time. The typical process width was set by the program and varied between images. For method of tracing there were three options to choose from: 'directional kernels' are good for images where you trace long processes that are more or less one continuous line, 'crawling rayburst' which is good for tracing processes that have variable borders, and 'voxel scooping' which is good for images that have a high contrast between the subject and the background. For this method we used voxel scooping because the microglia were stained with Iba1 and therefore had a much higher fluorescence compared to the background tissue. This in turn translates into a higher brightness value in Neurolucida 360 which the software uses to guide the tracing. After tracing the cleanup tool in Figure 3D was used to fix any problems found with the tracing such as incomplete processes (fragments).

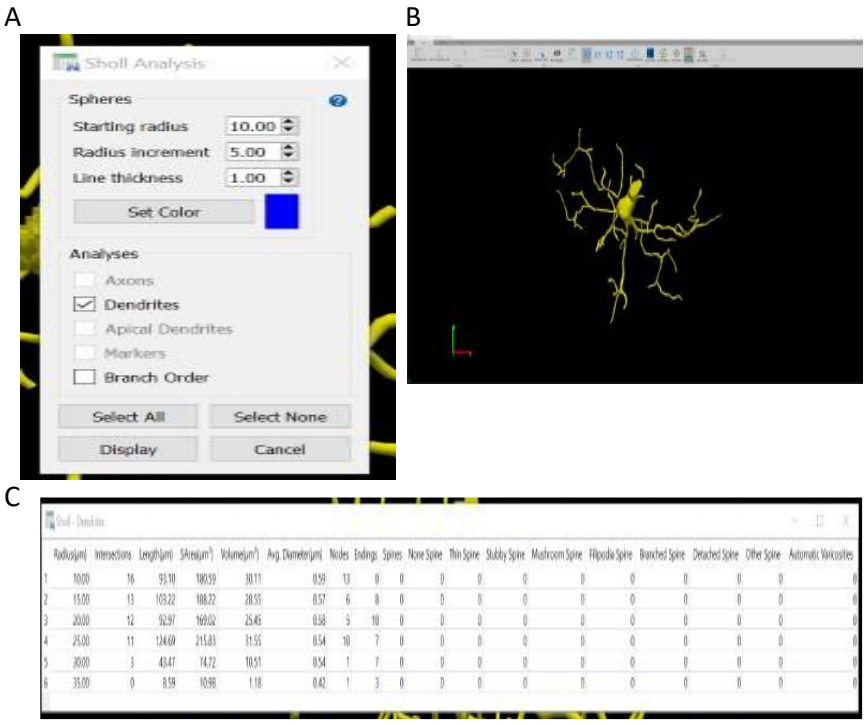

Figure 4. Analysis done in the Neurolucida® Explorer program after tracing in Neurolucida®360. (a) Sholl analysis settings used. (b) Finished reconstruction of target microglia. (c) Read out of Sholl analysis program.

Figure 4A shows the methodology for the Sholl analysis following the completed tracing of a microglial cell. For the starting radius 10 μm was chosen since the average size of the soma was a smaller value. Each group of data going outward was collected in $5\mu m$ increments until the program did not detect any tracings in the region. The analyses were set to dendrites to get the relevant measurements in order to determine microglia complexity.

In figure 4B we see the 3D special representation of the traced microglia using the accessory Neurolucida®Explorer program the comes with Neurolucida®360. For analysis, the program creates concentric rings $10\mu m$ out from the ceter of the soma, and at every

$5\mu m$ from there until there is no detectable tracing (e.g., 15, 20, 25, etc.). From this the program reports a data table as shown in Figure 4C where radius, intersections, length, surface area, volume, average diameter, nodes, and endings are calculated. By looking at these different variables and their fluctuations separately and in combination we can parse together an idea of the state of microglial activation in the brain as an effect of airborne pathogen inhalation.

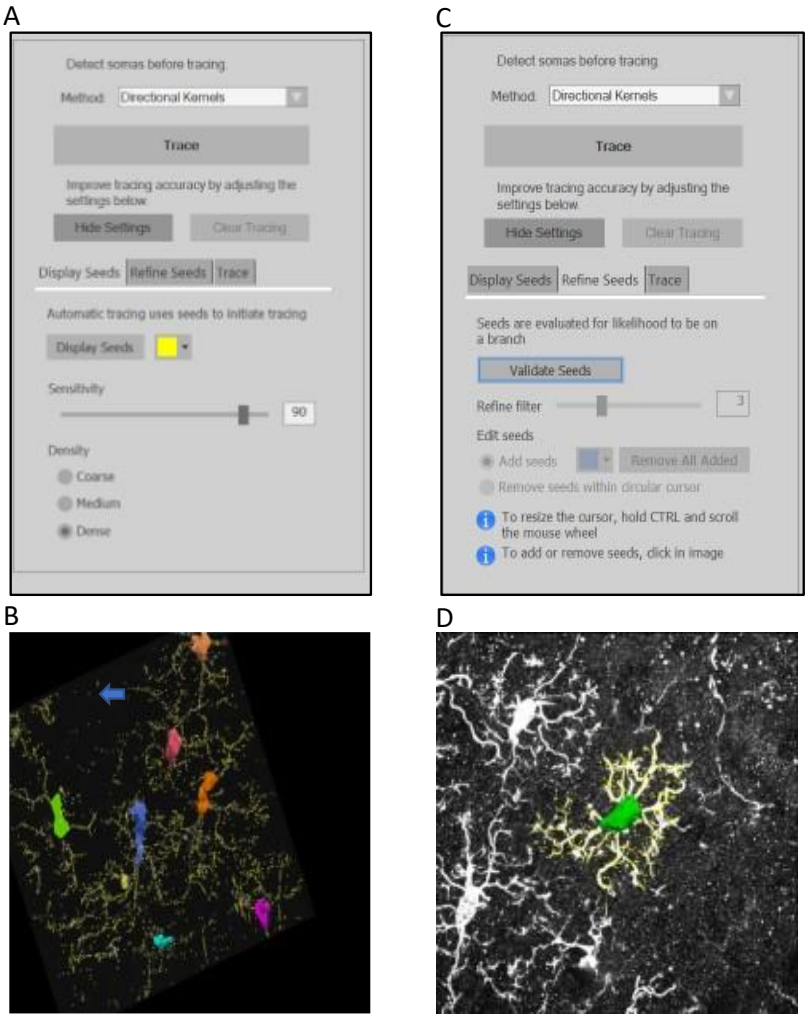

Figure 5. Process for seed detection and validation used in automatic tracings in Neurolucida®360. (a) Dialogue box setting the density of seeds displayed for the 3D reconstruction. (b) Example of 3D image after seeds are added with arrow indicating false positives. (c) Dialogue box used to validate and refine seed distribution to only target microglia. (d) Example of 3D image after seed refinement.

In Figure 5A is the screen to control seed density in the Neurolucida 360 program. Seeds refer to a guide point that the program uses for automatic tracing of the processes. The generation of seeds is dependent on the level of contrast between the subject and the background within a confined region of space. This parameter can be adjusted using the

sensitivity slider as shown in the figure in increments of 10. For our experiment, the slider was set to 80% as this value gave us the best results in terms of misses to hits to false positives. In the same figure the density refers to the total amount of seeds allowed within a defined space by the program, which was set to dense. This is because more seeds give a more accurate tracing in terms of the readout data that is collected as shown in Figure 4C.

In Figure 5B the completed seeding process is shown. Here it is shown that the numerous yellow circles in the tracing are seeds and that they coincide with the microglial processes which have their soma filled in through the process in Figure 2. However, most of the seeds will not be used for tracings mainly for two reasons. The first is that in each slice we only recorded the Sholl parameters of a single microglia to standardize our methods. Second not all seeds are generated on the microglial processes, as shown with the arrow in Figure 5B some seeds will be in various spots were there was a local increase in brightness compared to the background due to the nature of Iba1 staining. To rectify both, the seeds must be removed until just the target microglia remain seeded for the tracing program. To remove seeds, the options shown in Figure 5C are used. The refine filter is a feature that allows the program to change various seed parameters with the purpose of increasing/decreasing the requirements for the program to place a seed. For our experiment we used a refine filter level of 3. The outcome of this process is an image ready for automatic tracing as shown in Figure 5D.

A

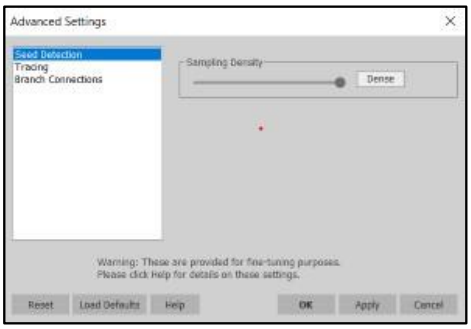

B

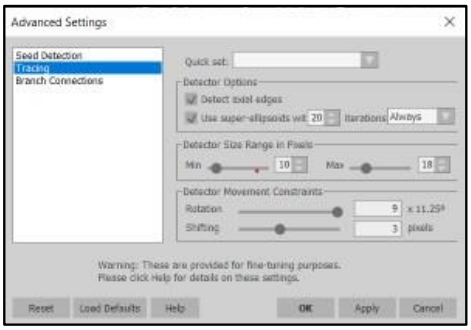

C

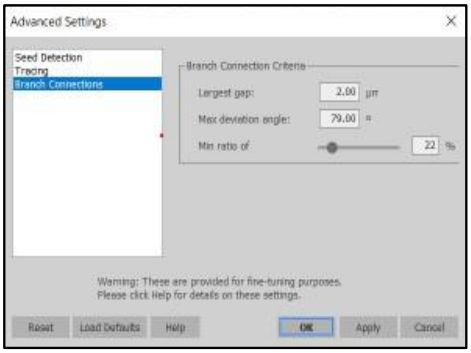

Figure 6. Array of dialogue boxes used for fine tuning microglial process tracing. (a) Options to change sampling density for seed detection. (b) Options to change different parameters of the program for automatic tracing of processes. (c) Settings to control the criteria for differentiation between a continuation of one branch process or the start of a new branch process.

Figure 6 shows the settings used for the automatic tracing of the microglia using the Neurolucida 360 program. In this methodology some of the parameters are set by the program, and some were manually set. In Figure 6A the first setting determines the

number of regions each 3D image is broken up into for seed placement. This was set to maximum to give us the most seeds to work with through the refinement process. The next settings in Figure 6B deal with the criteria to determine a branch within the program. The largest gap refers to the maximum amount of space allowed between two points on a branch to determine if the terminal point of a process. This parameter is autogenerated by the program from trial and error. Max deviation angle determines how far a process can deflect from a previous point on the branch and still be traced as the same process. The setting was set to the maximum degree of 79 to account for the fact that not all process follows a straight line and can deflect due to environmental factors. The third setting 'ratio of diameters' refers to the minimum amount of volumetric change a process can go through and still be considered the same process. For our methods this was set to 22%. In Figure 6B for detector options both detect axial edges and use super ellipsoids with 20 iterations are used for the automatic tracings. Both parameters are used to make sure that the processes traced reflect the actual volumetric measurements of the sample. The detector size range was set to 10-18 pixels as the program default. For detector movement controls only, rotation was changed from 3 to 9 x 11.25° to accommodate a wider range of possibilities for a process to shift. Shifting was left at the default 3 pixels.

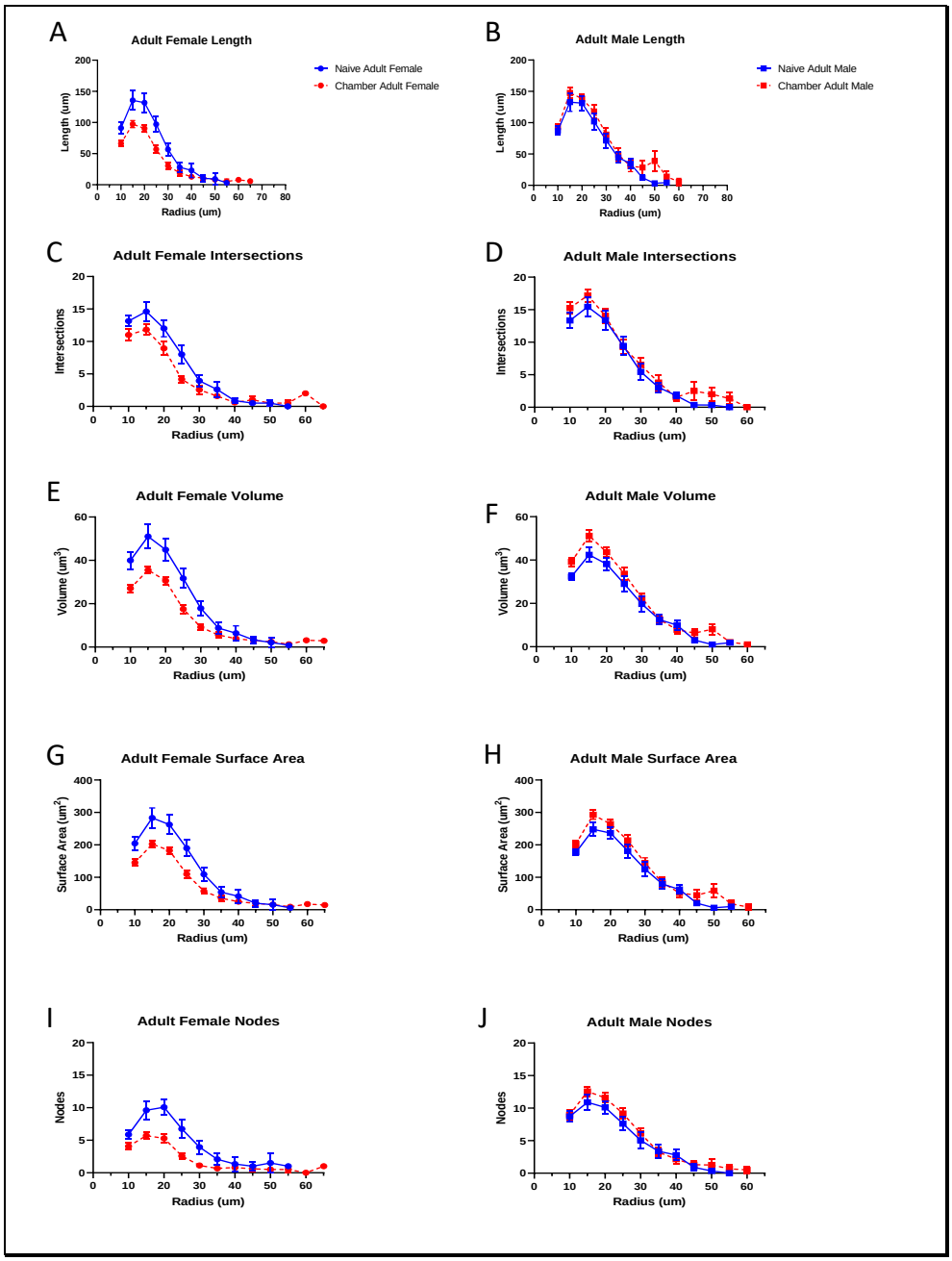

Figure 7. Sholl analysis of microglia cells from C57Bl/6J mice exposed for 7days to aerosolized *Alternaria* particulates or ambient air. (a, c, e, g, i) Data collected from adult female mice with naïve having N=2, n=15; and chamber having N=1, n=17. (b, d, f ,h, j) Data collected from adult male mice with naïve having N=2, n=18; and chamber having N=3, n=36. (a-j) Data collected included the parameters of process length, intersection number, volume, surface area, and node number. Data presented as the mean ± SEM using GraphPad Prism. (N= number of animals, n= number of microglial cells)

Figure 7 shows the graphed Sholl data from mice from each experimental condition. Note that the current graphs lack sufficient replicate power for significance for all conditions, but we can analyze what trends are presented within the data. Each microglia were traced using the automatic process in Neurolucida 360 software, and data was collected using the Neurolucida® Explorer software. Each graph shows the naïve condition (clean air) versus the treated condition (chamber air) for either males or females at 3 months of age. For each of the graphs the parameters are compared over the expanding radius for each microglial cell. Looking at the graphs some consistent trends are apparent. In the males we see that for most of the parameters the naïve adult males are lower than the chamber adult males. For females we saw the opposite trend where the chamber animals are lower on average than the naïve adult female mice. For males we see this trend reverse at around $40\mu m$ or greater where the microglia from chamber exposed mice have greater scores in surface area, intersections, volume, and length

The further out we analyze naturally microglial complexity decreases further out from the soma. As microglia are essentially biosensors in the brain, they survey a certain area of the surrounding tissue, and respond to the present stimuli. Naturally, complexity of the cell decreases the further out from the soma we look. In the data we can see that for both males and females the chamber mice have microglia that retain their complexity further out from the soma compared to the naïve mice. In addition, for most of the parameters in males the chamber microglia show to have a sudden increase of complexity at about $50\mu m$ before decreasing to zero.

Discussion

Environmental stimuli have been shown to modify brain microglial morphology to change to an activated state. The change has been shown to be graded along a spectrum of ramified to activated with microglia having the ability to shift states in a cycle (Jonas et al., 2012). In addition, LPS studies have shown that microglia will change their morphology into an activated state consisting of a reduction in the number of branches, path length, and as well as their length to volume ration with recovery after 10 days (Tejera et al., 2019).

Sex differences in immune response to has also been observed in other studies. Female mice have been observed to have a more robust response to inflammation compared to males. In an asthma model females respond with a more pronounced M2 macrophage phenotype and the response is also sensitive to estrogen signaling. Looking at ILC2 levels in an allergic airway inflammation also shows a disparity where females exhibit higher levels compared to males. This sex difference has also been found in an inhalation assay using Aspergillus fumigatus fungus; where females measured higher in antibody titers and fold change in granulocytes and lymphocytes with differences becoming more pronounced over a 28-day period (Keselman et al., 2017; Wang et al., 2020; Schaefer et al., 2020).

In our model system, 7-day Alternaria particulate inhalation exposure was shown to be sufficient to drive morphological change of microglia in adult C57Bl/6J mice. This can be seen when comparing the naïve condition to the chamber condition in female mice. In each of the parameters we measured by Sholl analysis we see that the chamber females

have less area under the curve indicating a change in morphology due to reactivity stimulated by the local environment, which also implicates less surveillance of the surrounding tissue by individual microglial cells. However, when we look at the male mice, we see no notable differences between the chamber and the naïve. A similar response of process retraction and thickening has been observed in other paradigms where the surround tissue suffered structural damage or in the presence of stronger antigen elements such as LPS (Jonas et al., 2012; Tejera et al., 2019).

Looking at the data we do see a rather consistent trend across sexes comparing the chamber mice microglia to the naïve. The chamber microglia trend to have processes that reach out longer than naïve microglia. Taking both this trend towards longer processes in conjunction with the differences within, and between both sexes for chambered and naïve microglia we hypothesize that this is a mixed response. It seems that the Alternaria was able to affect morphology of microglia to an atypical reactive state which appears as longer processes, and females were more prone to reach a further point of reactivity than the males with a more ameboid structure.

Whether this difference of reactivity between males and females is adaptive or maladaptive is unknown, but further research could tease out the differences between sexes.

References

1. "AAFA." Asthma and Allergy Foundation of America, www.aafa.org/allergy-facts/#:~:text=Allergic%20rhinitis%2C%20often%20called%20hay,million%20of%20the%20adult%20population.

2. "Most Recent National Asthma Data." Centers for Disease Control and Prevention, Centers for Disease Control and Prevention, 30 Mar. 2021, www.cdc.gov/asthma/most_recent_national_asthma_data.htm.

3. Bartemes, Kathleen R, and Hirohito Kita. "Innate and adaptive immune responses to fungi in the airway." The Journal of allergy and clinical immunology vol. 142,2 (2018): 353-363. doi:10.1016/j.jaci.2018.06.015

4. Bilbo S. D., Block C. L., Bolton J. L., Hanamsagar R., Tran P. K. (2018). Beyond infection—Maternal immune activation by environmental factors, microglial development and relevance for autism spectrum disorders. Exp Neurology, pii, S0014-4886(17)30176-0. doi:10.1016/j.expneurol.2017.07.002.

5. Cole T. B., Coburn J., Dao K., Roque P., Chang, Y. C., Kalia V., Guilarte T. R., Dziedzic J., Costa L. G. (2016). Sex and genetic differences in the effects of acute diesel exhaust exposure on inflammation and oxidative stress in mouse brain. Toxicology, 374, 1–9.

6. Eifan, A O, and S R Durham. "Pathogenesis of rhinitis." Clinical and experimental allergy : journal of the British Society for Allergy and Clinical Immunology vol. 46,9 (2016): 1139-51. doi:10.1111/cea.12780

7. Gabriel M. F., Postigo I., Tomaz C. T., Martínez J. (2016). Alternaria alternate allergens: Markers of exposure, phylogeny and risk of fungi-induced respiratory allergy. Environ Int, 89–90, 71–80

8. Gackiere F., Saliba L., Baude A., Bosler O., Strube C. (2011). Ozone inhalation activates stress-responsive regions of the CNS. J Neurochem, 117, 961–972

9. Guo R. B, Sun P. L, Zhao A. P, Gu J., Ding X., Qi J., Sun X. L., Hu G. (2013). Chronic asthma results in cognitive dysfunction in immature mice. Exp Neurol, 247, 209–217.

10. Heusinkveld H. J., Wahle T., Campbell A., Westerink R. H. S., Tran L., Johnston H., Stone V., Cassee F. R., Schins R. P. F. (2016). Neurodegeneration and neurological disorders by small inhaled particles. Neurotoxicology, 56, 94–106. https://www.ncbi.nlm.nih.gov/books/NBK27090/

11. Janeway CA Jr, Travers P, Walport M, et al. Immunobiology: The Immune System in Health and Disease. 5th edition. New York: Garland Science; 2001. Principles of innate and adaptive immunity.

12. Jayaraj R. L., Rodriguez E. A., Wang Y., Block M. L. (2017). Outdoor ambient air pollution and neurodegenerative diseases: The neuroinflammation hypothesis. Curr Environ Health Rep, 4, 166–179.

13. Jonas, Rahul A et al. “The spider effect: morphological and orienting classification of microglia in response to stimuli in vivo.” PloS one vol. 7,2 (2012): e30763. doi:10.1371/journal.pone.0030763

14. Keselman, Aleksander et al. “Estrogen Signaling Contributes to Sex Differences in Macrophage Polarization during Asthma.” Journal of immunology (Baltimore, Md. : 1950) vol. 199,5 (2017): 1573-1583. doi:10.4049/jimmunol.1601975

15. Klein B., Mrowetz H., Thalhamer J., Scheiblhofer S., Weiss R., Aigner L. (2016). Allergy enhances neurogenesis and modulates microglial activation in the hippocampus. Front Cell Neurosci, 10, 169. doi: 10.3389/fncel.2016.00169

16. Knutsen A. P., Bush R. K., Demain J. G., Denning D. W., Dixit A., Fairs A., Greenberger P. A., Kariuki B., Kita H., Kurup V. P., Moss R. B., Niven R. M., Pashley C. H., Slavin R. G., Vijay H. M., Wardlaw A. J. (2012). Fungi and allergic lower respiratory tract diseases. J Allergy Clin Immunol, 129(2), 280–291.

17. Kumar V., Abbas A. K., Aster J. C. (2014). Robbins & Cotran pathologic basis of disease (9th ed.). London, England: Elsevier Health Science

18. Levesque S, Taetzsch T, Lull M. E., Kodavanti U, Stadler K, Wagner A, Johnson J. A., Duke L, Kodavanti P, Surace M. J., Block M. L. (2011). Diesel exhaust activates and primes microglia: Air pollution, neuroinflammation, and regulation of dopaminergic neurotoxicity. Environ Health Perspect, 119, 1149–1155.

19. Ljubimova J. Y., Braubach O., Patil R., Chiechi A., Tang J., Galstyan A., Shatalova E. S., Kleinman M. T., Black K. L., Holler E. (2018). Coarse particulate matter (PM2.5-10) in Los Angeles Bain air induces expression of inflammation and cancer biomarkers in rat brains. Sci Rep, 8, 5708. doi: 10.1038/s41598-018-23885-3.

20. National Center for Health Statistics. Percentage of angina for adults aged 18 and over, United States, 2019. National Health Interview Survey. Generated interactively: May 25 2021 from https://wwwn.cdc.gov/NHISDataQueryTool/SHS_2019_ADULT3/index.html

21. National Center for Health Statistics. Percentage of ever having asthma for children under age 18 years, United States, 2019. National Health Interview Survey. Generated interactively: May 25 2021 from https://wwwn.cdc.gov/NHISDataQueryTool/SHS_2019_CHILD3/index.html

22. Peng, Xinze et al. "Continuous Inhalation Exposure to Fungal Allergen Particulates Induces Lung Inflammation While Reducing Innate Immune Molecule Expression in the Brainstem." ASN neuro vol. 10 (2018): 1759091418782304. doi:10.1177/1759091418782304

23. Pennock, Nathan D et al. "T cell responses: naive to memory and everything in between." Advances in physiology education vol. 37,4 (2013): 273-83. doi:10.1152/advan.00066.2013

24. Rosenbaum M. D., Van de Woude S., Johnson T. E. (2009). Effects of cage-change frequency and bedding volume on mice and their microenvironment. J Am Assoc Lab Animal Sci, 48, 763–773.

25. Schaefer, Andrea L et al. "Factors Contributing to Sex Differences in Mice Inhaling Aspergillus fumigatus." International journal of environmental research and public health vol. 17,23 8851. 28 Nov. 2020, doi:10.3390/ijerph17238851

26. Tejera, Dario et al. "Systemic inflammation impairs microglial Aβ clearance through NLRP3 inflammasome." The EMBO journal vol. 38,17 (2019): e101064. doi:10.15252/embj.2018101064

27. Vianello A., Caminati M., Crivellaro M., El Mazloum R., Snenghi R., Schiappoli M., Dama A., Rossi A., Festi G., Marchi M. R., Bovo C., Canonica G. W., Senna

G. (2016). Fatal asthma: Is it still an epidemic? World Allergy Organ J, 9, 42. doi: 10.1186/s40413-016-0129-9.

28. Wang, Cong et al. “Sex differences in group 2 innate lymphoid cell-dominant allergic airway inflammation.” Molecular immunology vol. 128 (2020): 89-97. doi:10.1016/j.molimm.2020.09.019